University of Wollongong
Research Online

Faculty of Science - Papers (Archive) | Faculty of Science, Medicine and Health

1-1-2012

Activity and molecular dynamics relationship within the family of human cholinesterase

Judith Peters
Universite Joseph Fourier

Marie Trovaslet
Institut de Recherche Biomédicale des Armées, France

Marcus Trapp
Universite Joseph Fourier

Florian Nachon
Institut de Recherche Biomédicale des Armées, France

Flynn Hill
University of Wollongong, flynn@uow.edu.au

See next page for additional authors

Follow this and additional works at: https://ro.uow.edu.au/scipapers

 Part of the Life Sciences Commons, Physical Sciences and Mathematics Commons, and the Social and Behavioral Sciences Commons

Recommended Citation

Peters, Judith; Trovaslet, Marie; Trapp, Marcus; Nachon, Florian; Hill, Flynn; Royer, Etienne; Gabel, Frank; van Eijck, Lambert; Masson, Patrick; and Tehei, Moeava: Activity and molecular dynamics relationship within the family of human cholinesterase 2012, 6764-6770.
https://ro.uow.edu.au/scipapers/4328

Research Online is the open access institutional repository for the University of Wollongong. For further information contact the UOW Library: research-pubs@uow.edu.au

Activity and molecular dynamics relationship within the family of human cholinesterase

Abstract

The temperature dependence of the dynamics of recombinant human acetylcholinesterase (hAChE) and plasma human butyrylcholinesterase (hBChE) is examined using elastic incoherent neutron scattering. These two enzymes belong to the same family and present 50% amino acid sequence identity. However, significantly higher flexibility and catalytic activity of hAChE when compared to the ones of hBChE are measured. At the same time, the average height of the potential barrier to the motions is increased in the hBChE, e.g. more thermal energy is needed to cross it in the latter case, which might be the origin of the increase in activation energy and the reduction in the catalytic rate of hBChE observed experimentally. These results suggest that the motions on the picosecond timescale may act as a lubricant for those associated with activity occurring on a slower millisecond timescale.

Keywords

dynamics, human, molecular, activity, family, within, relationship, cholinesterase

Disciplines

Life Sciences | Physical Sciences and Mathematics | Social and Behavioral Sciences

Publication Details

Peters, J., Trovaslet, M., Trapp, M., Nachon, F., Hill, F., Royer, E., Gabel, F., van Eijck, L., Masson, P., Tehei, M. (2012). Activity and molecular dynamics relationship within the family of human cholinesterase. Physical Chemistry Chemical Physics, 14 (19), 6764-6770.

Authors

Judith Peters, Marie Trovaslet, Marcus Trapp, Florian Nachon, Flynn Hill, Etienne Royer, Frank Gabel, Lambert van Eijck, Patrick Masson, and Moeava Tehei

This journal article is available at Research Online: https://ro.uow.edu.au/scipapers/4328

PCCP

Dynamic Article Links
View Online

Cite this: *Phys. Chem. Chem. Phys.*, 2012, **14**, 6764–6770

www.rsc.org/pccp

PAPER

Activity and molecular dynamics relationship within the family of human cholinesterases

Judith Peters,*[abc] Marie Trovaslet,[d] Marcus Trapp,†[ab] Florian Nachon,[d] Flynn Hill,[f] Etienne Royer,[ab] Frank Gabel,[c] Lambert van Eijck,‡[b] Patrick Masson[cd] and Moeava Tehei[ef]

Received 30th November 2011, Accepted 16th February 2012
DOI: 10.1039/c2cp23817a

Published on 17 February 2012 on http://pubs.rsc.org | doi:10.1039/C2CP23817A
Downloaded by University of Wollongong on 22 August 2012

The temperature dependence of the dynamics of recombinant *human* acetylcholinesterase (*h*AChE) and plasma *human* butyrylcholinesterase (*h*BChE) is examined using elastic incoherent neutron scattering. These two enzymes belong to the same family and present 50% amino acid sequence identity. However, significantly higher flexibility and catalytic activity of *h*AChE when compared to the ones of *h*BChE are measured. At the same time, the average height of the potential barrier to the motions is increased in the *h*BChE, *e.g.* more thermal energy is needed to cross it in the latter case, which might be the origin of the increase in activation energy and the reduction in the catalytic rate of *h*BChE observed experimentally. These results suggest that the motions on the picosecond timescale may act as a lubricant for those associated with activity occurring on a slower millisecond timescale.

1 Introduction

Two different types of cholinesterases (ChEs) are found in mammalian organisms and can hydrolyse the neurotransmitter acetylcholine: acetylcholinesterase (AChE) and butyrylcholinesterase (BChE). These enzymes also hydrolyse numerous other non-physiological esters. AChE is mainly located at the neuromuscular junctions and the cholinergic synapses, whereas BChE can be found in the plasma, in glial cells in the central nervous system, and several tissues. Although AChE is a key enzyme in the nervous system to terminate neurotransmission at cholinergic synapses, the physiological function of BChE is not yet known. BChE acts as a backup for AChE in the nervous system and as an endogenous bioscavenger for esters that are potential inhibitors of AChE.[1] In fact, an abrupt blockade of acetylcholine-mediated neurotransmission is lethal, whereas the inhibition of BChE or the absence of BChE (homozygous individuals for silent BChE genes) in humans has no known deleterious effects.[2,3]

The first crystallographic structure of *Torpedo californica* AChE (*Tc*AChE) was resolved in 1991[4] and for a long time most of the studies were performed on *Tc*AChE. Its structure revealed surprising features: the active site is located at the bottom of a deep and narrow gorge lined by 14 conserved aromatic residues. Due to the restrictive dimensions of the active site gorge of *Tc*AChE (20 Å deep, diameter ≈ 5 Å), the substrate hydrolysis takes place in a closed space virtually isolated from the bulk solvent.[5] In parts, the gorge is so narrow that only water molecules can pass through it, but neither substrates nor inhibitors would have access to the active site if the enzyme was rigid.[6] The structure of *human* BChE (*h*BChE) was solved in 2003 by Nicolet *et al.*[7] The active site gorge of *h*BChE is much larger than its *Tc*AChE counterpart (∼500 Å^3 *vs.* 300 Å^3). Among the 14 aromatic residues that line the active site gorge of *Tc*AChE and determine its narrow path, six are substituted in *h*BChE by smaller aliphatic or even polar residues. These residues account for most of the differences in catalytic properties observed between the two enzymes.[3] The structure of the free *human* AChE (*h*AChE) was not known for a long time because its crystallisation was challenging. The difficulty in growing the crystals was suggested to be related to the high intrinsic flexibility of the enzyme. Later, Kryger *et al.*[8] succeeded to solve the structure of the *h*AChE complexed with fasciculin-II, a snake neurotoxin, which may decrease the flexibility of *h*AChE and increase its thermostability,[9]

[a] *Université Joseph Fourier, UFR PhITEM, F-38041 Grenoble Cédex 9, France. E-mail: peters@ill.fr; Fax: +33 4 76 20 76 88; Tel: +33 4 76 20 75 60*
[b] *Institut Laue Langevin, F-38042 Grenoble Cédex 9, France*
[c] *Institut de Biologie Structurale J.-P. Ebel, UMR 5075, CNRS-CEA-UJF, F-38042 Grenoble Cédex 9, France*
[d] *Institut de Recherches Biomédicales des Armées, antenne de La Tronche, France*
[e] *Australian Institute of Nuclear Science and Engineering (AINSE), Menai, NSW, Australia*
[f] *School of Chemistry and Centre for Medical Bioscience, University of Wollongong, Wollongong, NSW 2522, Australia*
† Current address: Applied Physical Chemistry, University of Heidelberg, 69120 Heidelberg, Germany and Helmholtz Zentrum Berlin, 14109 Berlin, Germany.
‡ Current address: Faculty of Applied Sciences, Delft University of Technology, 2628 CJ Delft, The Netherlands.

This journal is © the Owner Societies 2012

Published on 17 February 2012 on http://pubs.rsc.org | doi:10.1039/C2CP23817A
Downloaded by University of Wollongong on 22 August 2012

and therefore ease its crystallisation. The structure of the free *h*AChE was only determined recently by Dvir *et al.*[10] The volumes of the active sites of *h*AChE and *Tc*AChE are similar and the 14 aromatic residues in the active site gorge of *h*AChE are also conserved. *Tc*AChE, *h*AChE and *h*BChE have a high structural identity (about 53%) with a very low structural root mean square deviation (about 1 Å).

The peptide sequences are 54% homologous among the species of ChEs, and even more for the catalytic subunit.[3,7] However, *h*BChE has a higher number of N-glycosylation chains than *h*AChE (9 against 4), representing a sugar content of 25% of its mass against 9% for *h*AChE. Glycosylation is known to alter folding, stability and the dynamical properties of ChEs, but not their catalytic properties.[11] AChE and BChE are highly polymorphic depending on the environment and the specific species. In solution, recombinant *human* AChE presents a mixture of monomers and dimers, which are sometimes also arranged in tetramers. *Human plasma* BChE is naturally tetrameric.

AChE is a very fast enzyme, especially for a serine hydrolase, functioning at a rate approaching that of a diffusion-controlled reaction. The high speed of the enzyme is essential for rapid functioning of cholinergic synapses, with a turnover of 10^3–10^4 s^{-1}. The catalytic rate of BChE is about ten times smaller.[2] The question whether differences in activity are reflected in the sub-nanosecond dynamics is still an unresolved matter.[12] Shafferman *et al.*[13] argued, however, that the active site seems to require a certain balance between rigidity to stabilize the catalytic triad, and flexibility for binding the different AChE ligands.

In the present work, the combined analysis of neutron data on sub-nanosecond dynamics, on the one hand, with activity data, on the other, for *h*AChE and *h*BChE, established complex correlations between dynamics and function. We discuss these observations in terms of the effects of activation free energy barrier increasing on the mechanisms for the catalysed reactions of the human ChEs. In addition, results suggest that overall thermal dynamics occurring on the sub-nanosecond timescale has an influence on the much slower millisecond timescale of the catalytic activity.

2 Materials and methods

2.1 Production, purification and characterization of cholinesterases

Homemade pGS vector carrying cDNA of *h*AChE and the glutamine synthetase gene marker was expressed in Chinese hamster ovary cells (CHO-K1 cells). The cells were stably transfected using JetPEI transfection protocol without modification (Polyplus transfection, France). Selective pressure was provided by methionine sulfoximide (MSX—50 μM). The highest producing clone was maintained in BioWhittaker UltracultureTM medium (Lonza, Belgium) also containing MSX. The cells were first grown in Petri dishes, in culture flasks and then were expanded for high volume culture in 1 L roller bottles. The enzyme, secreted into the culture medium, was first precipitated by addition of 80% saturation ammonium sulfate. The protein pellet was suspended, extensively dialyzed against ammonium acetate buffer (25 mM, pH 7.0) and loaded onto an affinity chromatography column (Sepharose-4B/procainamide). After extensive washing (using ammonium acetate buffer containing 0.5 M NaCl), *h*AChE was eluted with ammonium acetate buffer containing 1 M NaCl + 0.5 M tetramethylammonium iodide + 1 mM decamethonium chloride. The fractions containing the highest *h*AChE activity were pooled and concentrated (using a Centricon-30 ultrafiltration microconcentrator from Amicon, Millipore, USA). Enzyme concentration was determined from its absorbance at 280 nm using a molar extinction coefficient of 1.7 for 1 mg mL^{-1} of protein.[14] *h*BChE used for kinetic studies was purified from human plasma as described in ref. 15. Cholinesterases activity measurements were carried out at 25 °C according to the Ellman method[16] using 1 mM acetylthiocholine (ATC (for *h*AChE)) or butyrylthiocholine (BTC (for *h*BChE)) as substrate and 0.5 mM 5–5′-dithio-bis(2-nitrobenzoic acid) (DTNB) in 0.1 M phosphate buffer pH 7.0. As for *h*BChE, the *h*AChE sample was assayed before and after the neutron scattering experiments: activity of the batch was not significantly reduced by the neutron scattering experiments.

2.2 Kinetic studies

The *h*AChE and *h*BChE activities were determined at various temperatures from 7 to 38 °C. Reaction rates (k) were measured at intervals of 1–2 °C, with the same enzyme concentration (0.17 nM) and the optimum substrates concentration (1 mM ATC or BTC) in 0.1 M phosphate buffer pH 7.0 containing 0.1% albumin. Observed reaction rates were corrected for spontaneous substrate hydrolysis. Arrhenius plots were obtained by plotting $\ln(k)$ *vs.* $1/T$, where T is the absolute temperature. Activation energies ($E_a^{\ddagger}$) were calculated from the linear parts of the Arrhenius plots, below and above transition temperature (T_t). The enthalpies ($\Delta H^{\ddagger}$) and the entropies ($\Delta S^{\ddagger}$) of activation were, respectively, obtained from the slope and the intercept of the Eyring plot ($\ln(k)/T$ *vs.* $1/T$). The Gibbs energies of activation ($\Delta G^{\ddagger}$) were defined as $\Delta G^{\ddagger} = \Delta H^{\ddagger} - T\Delta S^{\ddagger}$.

2.3 Sample preparation for neutron scattering

*h*BChE used for dynamics studies was prepared as described in Gabel *et al.*[15] Special care was taken for the sample preparation of *h*AChE in order to respect exactly the same protocol and to exclude any spurious effect due to that. So, the *h*AChE sample was prepared as follows: about 130 mg of *h*AChE was dialyzed against 25 mM ammonium acetate dissolved in D_2O, pD 7.0. Since the buffer is completely volatile, a 12 hours freeze drying at 220 K under vacuum resulted in salt free protein powder. The lyophilized powder was placed in an aluminium sample container matching the size of the neutron beam available on the instrument. The sample was dried for 12 hours at atmospheric pressure over P_2O_5 and weighed. The measured weight was taken as its dry weight (h = 0 g D_2O g^{-1} dry powder, denoted by g/g). For neutron experiments, the sample was then hydrated by vapour exchange over D_2O, at ambient temperature, in a desiccator. A final water content of about 0.4 g/g for the sample was achieved. To verify that no loss of material had occurred and that the hydration state

Published on 17 February 2012 on http://pubs.rsc.org | doi:10.1039/C2CP23817A
Downloaded by University of Wollongong on 22 August 2012

was the same, samples were weighed before and after the neutron scattering experiments. No losses were detected for any sample.

2.4 Elastic incoherent neutron scattering

Both experiments were performed on the IN16 backscattering spectrometer at the ILL, the experiment on *h*BChE was realized in 2003[15] and the one on *h*AChE in 2009. No substantial modifications were undertaken in that period on the instrument. The data treatment was made using the ILL program LAMP (Lamp). We reanalysed the data from Gabel *et al.*[15] with this program, and exactly the same results for *h*BChE were obtained compared to what was published. A neutron scattering experiment with angular and energy resolution measures the double differential scattering cross section $\frac{d^2\sigma}{d\Omega dE}$, which is the number of neutrons scattered per second into the solid angle $d\Omega$ in the direction of the scattering vector $\vec{k}'$ with an energy in the interval between E and $E + dE$, normalized by the incident neutron flux Φ. It can be split into two parts: the coherent and the incoherent scattering. Coherent scattering carries information on the structure of a material and on the collective dynamics of the atoms, whereas incoherent scattering contains information on the individual atomic dynamics. It can be interpreted as a superposition of neutron waves that were scattered from the same nucleus at different times. The experimentally accessible time range is determined by the energy resolution $\Delta\omega$ of the instrument. The double differential scattering cross section is connected to the scattering function $S(\vec{Q}, \omega)$ *via*

$$\frac{d^2\sigma}{d\Omega dE} = N\frac{\sigma_{coh}}{4\pi}\frac{k'}{k}S(\vec{Q},\omega)_{coh} + N\frac{\sigma_{inc}}{4\pi}\frac{k'}{k}S(\vec{Q},\omega)_{inc}, \quad (1)$$

where σ_{coh} and σ_{inc} are the total coherent and incoherent scattering cross sections. k and k' are the absolute values of the incoming and scattered wave vectors of the neutron, respectively. $\vec{Q}$ is the scattering vector defined as $\vec{Q} = \vec{k}' - \vec{k}$ and $\hbar\omega = \frac{\hbar^2}{2m_n}(k'^2 - k^2) = E' - E$ the energy transfer between the incident and scattered neutron for elastic scattering, thus $\omega = 0 \pm \Delta\omega$.

This is due to the hydrogen incoherent scattering cross section which is one order of magnitude larger than that of all other elements usually occurring in biological matter, and also of its isotope deuterium.[17] The technique probes average protein dynamics because hydrogen atoms are uniformly distributed in the protein. *h*AChE contains a high proportion of hydrogen, 4673 of a total of 9470 atoms. The incoherent cross section of the hydrogen atoms thus corresponds to 99.8% of the total incoherent cross section and to 92.6% of the total scattering of the sample (without the D_2O hydration layer). *h*BChE contains 4126 hydrogen atoms of a total of 8346 atoms. It accounts for 99.9% of its incoherent signal and for 92.7% of the total scattering. An atomic mean square displacement (MSD) value $\langle u^2\rangle$ for averaged single particle motions can be calculated from the Q-dependence of the elastic part of the dynamic structure factor, $S(Q, 0 \pm \Delta\omega)$. Using the Gaussian approximation,[18] which assumes that the distribution of the atoms around their average position follows a Gaussian distribution, one gets:

$$S(Q, 0 \pm \Delta\omega) \approx \exp(-2W), \quad (2)$$

where

$$W = \tfrac{1}{6}Q^2\langle u^2\rangle. \quad (3)$$

As Q approaches zero, the approximation is strictly valid for any motion localized in the length-time window of the spectrometer, and it holds up to $\sqrt{\langle u^2\rangle Q^2} \approx \sqrt{2}$.[19,20]

Finally the average mean square displacements can be obtained from the slope of the logarithm of the scattered intensities according to

$$\langle u^2\rangle = -3\frac{\partial \ln S(Q, 0 \pm \Delta\omega)}{\partial Q^2}. \quad (4)$$

The Q-domain used for fitting the data was 0.43 $Å^{-1} \leq Q \leq$ 1.06 $Å^{-1}$.

3 Results

3.1 Effects of temperature on elastic incoherent neutron scattering

All measurements were carried out on the backscattering spectrometer IN16 at the Institute Laue-Langevin (ILL)/France on powder of *h*AChE hydrated at 0.4 g D_2O/g of protein. This corresponds to a full protein hydration and ensures the fully functioning of the enzyme.[21–23] Elastic incoherent scattering data were collected with an energy resolution of 1 μeV and analysed in a scattering vector range of 0.43 $Å^{-1} \leq Q \leq$ 1.06 $Å^{-1}$, corresponding to a space-time measurement window of 1 Å in 1 ns. Atomic mean square displacements (MSDs or $\langle u^2\rangle$) were extracted from elastic incoherent neutron scattering (EINS) data as described in Materials and methods. Fig. 1 shows the MSDs of *h*AChE and *h*BChE as a function of temperature. At low temperatures, the MSDs of both samples are similar and increase linearly with temperature. There is a significant deviation from linearity of $\langle u^2\rangle$ for $T > 175$ K and $T > 225$ K in the *h*AChE and *h*BChE samples, respectively. This deviation,

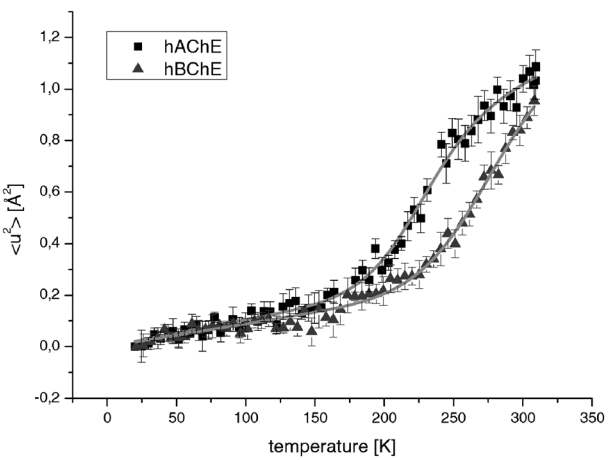

Fig. 1 MSDs of *h*AChE (black squares) and *h*BChE (blue triangles) with corresponding frequency window model fits (red lines). For *h*BChE, the MSDs were reanalysed using the data from Gabel *et al.*[15]

This journal is © the Owner Societies 2012

Published on 17 February 2012 on http://pubs.rsc.org | doi:10.1039/C2CP23817A
Downloaded by University of Wollongong on 22 August 2012

named dynamical transition, was already observed on other proteins.[24,25] Above its dynamical transition temperature, the MSD values of *h*AChE are starting to be larger than the ones of *h*BChE implying that *h*AChE is therefore more flexible than *h*BChE. The magnitude of the change above each dynamical transition temperature is similar for both proteins up to about 260 K where it starts to decrease for *h*AChE, only. This latter feature can be explained by the limitation of the instrumental resolution in relation to the measurement of large-scale motions[15] or by the relaxation frequencies that move into another instrumental range.[26] Different models (Bicout and Zaccai[27] and Gabel *et al.*[28]) were investigated to describe these behaviours (data not shown), but they were not very successful as the resolution dependency was not taken explicitly into account. The authors thus used the frequency-window model (FWM)[26] that can describe both the temperature and timescale dependences of $\langle u^2 \rangle$. Assuming activated dynamics, the transition would be determined by the barriers between energy minima. The corresponding equation used for fitting the MSDs within the FWM is given by:

$$\langle u^2 \rangle_{\mathrm{FWM}} = \langle u^2 \rangle_{\mathrm{fast}} + \langle u^2 \rangle_{\mathrm{slow}} \left(1 - \frac{2}{\pi} \arctan \frac{\Delta\omega}{\kappa_{\mathrm{FWM}}} \right), \quad (5)$$

where $\langle u^2 \rangle_{\mathrm{fast}}$ and $\langle u^2 \rangle_{\mathrm{slow}}$ correspond to fast and slow contributions to the mean square displacement in the instrumental resolution, respectively. $\Delta\omega = 0.5\ \mu\mathrm{eV} \cong 7.595 \times 10^8\ \mathrm{s}^{-1}$ is the half-width at half maximum of the elastic instrumental resolution function of IN16 and κ_{FWM} represents the long-time relaxation frequency corresponding to the characteristic time scale of the underlying process. $\langle u^2 \rangle_{\mathrm{fast}}$ is assumed to depend linearly on temperature as $\langle u^2 \rangle_{\mathrm{fast}} = \alpha T$ and can be obtained by fitting the data at low temperatures with a straight line. This approximation may not always been justified depending on the energy resolution, Q range and the protein hydration used, as shown by Pieper *et al.*[29] and Wood *et al.*[30] As our data are well fitted within the experimental errors by a straight line, where the results for both proteins are similar, we have then chosen this approach. $\langle u^2 \rangle_{\mathrm{slow}}$ is a fit parameter taking into account slow contribution due to diffusive processes.[26] Assuming Arrhenius behaviour for FWM, it can be expressed as:

$$\kappa_{\mathrm{FWM}}(T) = a\mathrm{e}^{-E_{\mathrm{a}}/RT}, \quad (6)$$

where a is a pre-exponential factor, E_{a} the dynamic activation energy, R the ideal gas constant and T the temperature. The parameter a was set to a value of $1 \times 10^{12}\ \mathrm{s}^{-1}$ for all samples. When this parameter was not fixed during the fitting procedure, we obtained very similar results but the fit was unstable *e.g.* the errors became larger than the extracted values. As the exact value had almost no influence on the other independent parameters, we thus fixed it to this value, which is characteristic for vibrational frequencies.[31] The resulting fits of the elastic data of the *h*AChE and *h*BChE samples are shown in Fig. 1 and the corresponding fitting parameters are summarized in Table 1.

The frequency-window model takes into account the temperature dependence of the MSDs for both proteins including the motions at low temperature, the dynamical transitions and the kink of the *h*AChE data starting around 260 K. The fast motions in the low T regime, $\langle u^2 \rangle_{\mathrm{fast}} = \alpha T$, were found to be comparable for *h*AChE and *h*BChE. The $\langle u^2 \rangle_{\mathrm{slow}}$ values are comparable and are close to the highest MSD values for both proteins, in agreement with Becker's publication.[26] The dynamical transition temperature is shifted up by 50 K for *h*BChE with a dynamical energy activation barrier 1.2 times higher than the one of *h*AChE (Table 1).

Table 1 Values obtained from fitting eqn (5) to the mean square displacements of *h*AChE and *h*BChE for data measured on IN16

Parameters	*h*AChE	*h*BChE
α/Å^2 K^{-1}	0.00101 ± 0.00004	0.0009 ± 0.00003
$\langle u^2 \rangle_{\mathrm{slow}}$/Å^2	0.83 ± 0.03	1.00 ± 0.09
a/s^{-1}	1×10^{12}	1×10^{12}
E_{a}/kJ mol^{-1}	14.17 ± 0.16	17.09 ± 0.33

3.2 Effects of temperature on enzyme activity

*h*AChE and *h*BChE kinetic measurements[32] were performed under the same conditions, between 7 and 38 °C. Whatever the temperature explored, the activity of *h*AChE is higher than that obtained for *h*BChE (Fig. 2a). As previously reported,[33–35] the Arrhenius plots (Fig. 2b) are biphasic, showing breaks at a transition temperature (T_{t}) of 21 °C for *h*BChE and 25 °C for *h*AChE. Activation energies ($E_{\mathrm{a}}^{\ddagger}$) can be calculated from the slopes of Arrhenius plots (Fig. 2b), both below and above the transition temperatures (Fig. 2b and Table 2). These $E_{\mathrm{a}}^{\ddagger}$ correspond to the amount of energy needed to be added to the enzyme + reactants to yield enzyme + products, passing through an activated complex. For both enzymes, $E_{\mathrm{a}}^{\ddagger}$ decline at high temperatures. This feature was already observed in *Electrophorus electricus* AChE.[36] As expected, $E_{\mathrm{a}}^{\ddagger}$ values are higher for *h*BChE (48.0 ± 2.3 kJ mol^{-1} and 36.4 ± 1.3 kJ mol^{-1} below and above T_{t}) than for *h*AChE (30.1 kJ mol^{-1} and 11.5 kJ mol^{-1} below and above T_{t}) with ratios of 1.6 and 3.1, respectively, below and above T_{t}. From the Eyring plots (Fig. 2c), we extracted the enthalpy ($\Delta H^{\ddagger}$), the entropy ($\Delta S^{\ddagger}$) and the free energy ($\Delta G^{\ddagger}$) of activation (Fig. 2c and Table 2). All values of $\Delta H^{\ddagger}$, $\Delta S^{\ddagger}$, $\Delta G^{\ddagger}$ are lower for *h*AChE compared to those of *h*BChE. *h*AChE has also a fairly larger negative entropy of activations compared to *h*BChE. This may suggest a very loose structure for *h*AChE and the loss of degrees of freedom of this protein and the reactant water in the transition state.

4 Discussion and conclusions

Taking the parameters obtained by the fits for κ_{FWM}, one can represent the relaxation frequencies for both enzymes (Fig. 3) as a function of the temperature according to eqn (6). In Fig. 3, the instrumental relaxation frequency limit is represented by a horizontal straight line. If the relaxation frequencies of the motions are above this limit, the motions are then too fast to be well resolved by the instrument. For both proteins and at low temperature, the frequencies are very small and the movements lie thus within the instrumental relaxation limit. As the activation energy is higher for BChE than for AChE, more thermal energy is necessary for BChE to overcome the barrier and thus the increase of the relaxation frequency values starts for higher temperature. The relaxation frequency curve of *h*AChE crosses the instrumental relaxation limit around 250 K, which is consistent with the temperature at which the kink of the *h*AChE MSDs is observed in Fig. 1, suggesting therefore that the origin

Published on 17 February 2012 on http://pubs.rsc.org | doi:10.1039/C2CP23817A
Downloaded by University of Wollongong on 22 August 2012

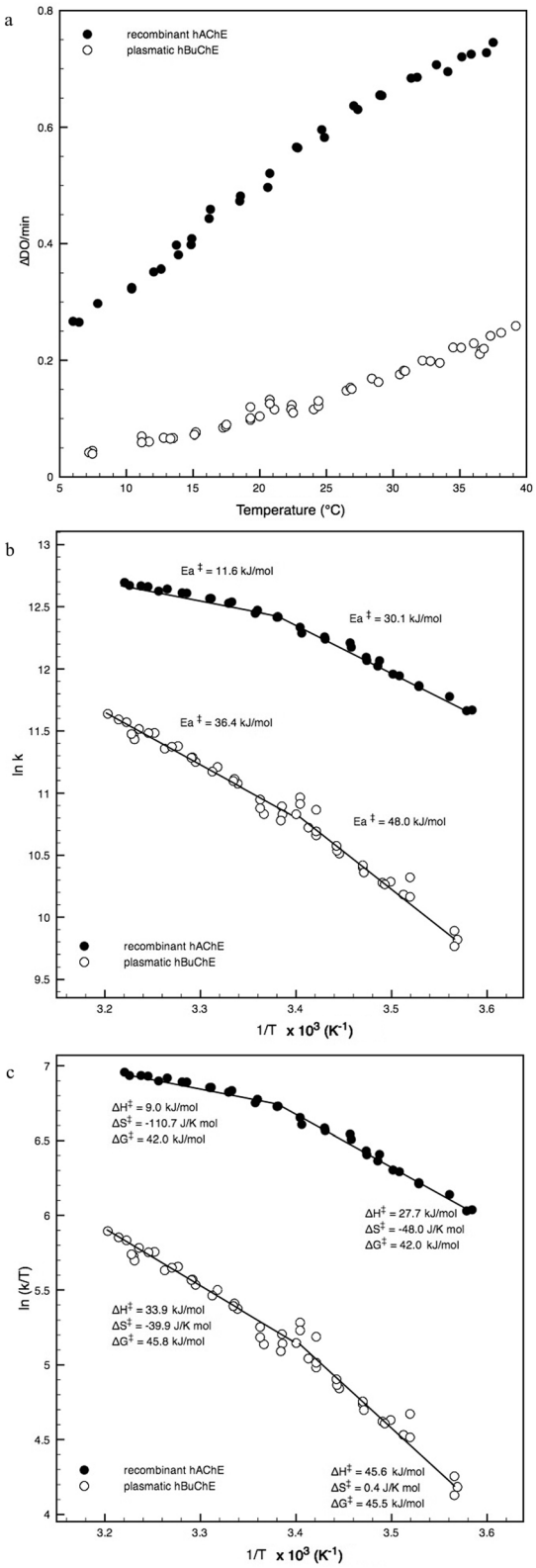

Fig. 2 Activity (a), Arrhenius (b) and Eyring (c) plots of *h*AChE (full circles) and *h*BChE (empty circles) catalysed hydrolysis of ATC or BTC, respectively.

of this kink is due to the fact that the frequencies of the *h*AChE motions become too fast to be measured on IN16. Conversely, this limit is only reached at about 330 K for *h*BChE, well above the temperature range investigated on IN16. This is then in agreement with the fact that we did not observe this kink of the MSDs in the case of *h*BChE. This observation also suggests that faster motions are becoming important for *h*AChE and may contribute to its higher catalytic activity. The extracted dynamic activation energies E_a are in the same order with other values in the literature for biological molecules such as bovine pancreatic trypsin inhibitor (BPTI)[26] and haemoglobin.[37] The activation energy for the motions is higher for *h*BChE than for *h*AChE, in agreement with the fact that *h*AChE is globally more flexible than *h*BChE. The dynamical activation energy of *h*BChE is about 1.2 times higher than the value found for *h*AChE. A similar activation energy ratio was found for the thermodynamic parameters extracted from the activity measurements at low temperatures before the transition temperature (corresponding to about the higher temperature probed in the dynamics study), suggesting thus a strong correlation between increasing flexibility and increasing activity in the case of this family of enzymes.

Despite the high structural affinity of both proteins and more than 50% amino acid sequence identity, their molecular dynamics are different. We then explored the potential impact caused by the oligomerization and glycosylation state on the dynamics. Using IN16, Gabel *et al.*[15] compared the dynamics of the tetrameric *h*BChE and dimeric native *Drosophila melanogaster* acetylcholinesterase (*Dm*AChE) and no difference in the MSDs could be observed over the whole temperature range for these two proteins. In addition, neutron spectroscopy studies[38,39] suggested that oligomerization, which supposes protein domain motions, happens at much longer time scales (up to a few hundred ns), which are not accessible within the present instrumental resolution. Thus we considered that oligomerization could not be at the origin of the important dynamics difference between the two proteins on IN16 using elastic neutron scattering. The glycosylation state differs significantly for both enzymes investigated here. *h*BChE contains 9 *N*-glycans against 4 for *h*AChE, bound covalently to an asparagine residue at the surface of the enzyme. The *N*-glycans form chains and interact rather poorly with the protein. The number and presence of NANA (*n*-acetylneuraminic acid) residues at termini of attached *N*-glycans was found to be strongly correlated with the circulatory residence time in blood, but not with the catalytic activity.[40,41] Again comparing *h*BChE and *Dm*AChE,[15] which has 4 glycosylation sites as *h*AChE, no difference was detectable for the dynamics between both proteins. One can then ask why we do have a difference of dynamics between *h*BChE and *h*AChE and none between *h*BChE and *Dm*AChE. One of the answers is certainly linked to the difference of activities between these two pairs of proteins. Indeed, at 25 °C the calculated ratio of k_{cat} (*Dm*AChE/*h*BChE) for hydrolysis is 1.8[15] and the corresponding ratio for (*h*AChE/*h*BChE) is about 5 (Fig. 2a).

The catalytic activity is much higher for *h*AChE than for *h*BChE (compare Fig. 2a) and strongly correlated to the higher flexibility of *h*AChE when compared to that of *h*BChE. The latter feature is translated through the dynamical activation energy E_a, which is about 1.2 times smaller for *h*AChE than for *h*BChE. This is significant when the two enzymes used in this study are from the same family with a high structural identity. All the values of $\Delta H^{\ddagger}$, $\Delta S^{\ddagger}$, $\Delta G^{\ddagger}$ are lower for *h*AChE with respect to those of *h*BChE. As expected, the values of $\Delta H^{\ddagger}$ are

 This journal is © the Owner Societies 2012

View Online

Table 2 Thermodynamic activation parameters derived from the activity, Arrhenius and Eyring plots (Fig. 2). The free energy of activation for hydrolysis of BTC (for *h*BChE) or ATC (for *h*AChE) was calculated for $T = 298$ K (25 °C). The $E_a^{\ddagger}$ values for each enzyme were obtained using their respective optimum substrates, homologous from the same series of thiocholine esters

Protein	Transition temperature (T_t/°C)	Activation energies ($E_a^{\ddagger}$/kJ mol^{-1})		Enthalpy of activation ($\Delta H^{\ddagger}$/kJ mol^{-1})		Entropy of activation ($\Delta S^{\ddagger}$/kJ mol^{-1})		Free energy of activation ($\Delta G^{\ddagger}$/kJ mol^{-1})	
		Below T_t	Above T_t	Below T_t	Above T_t	Below T_t	Above T_t	Below T_t	Above T_t
*h*BChE	21	48.0 ± 2.3	36.4 ± 1.3	45.6 ± 2.3	33.9 ± 1.3	0.4 ± 0.02	−39.9 ± 1.1	45.5 ± 2.4	45.8 ± 1.4
*h*AChE	25	30.1 ± 0.8	11.6 ± 0.7	27.7 ± 0.8	9.0 ± 0.7	−48.0 ± 0.9	−110.7 ± 2.9	42.0 ± 0.8	42.0 ± 0.7

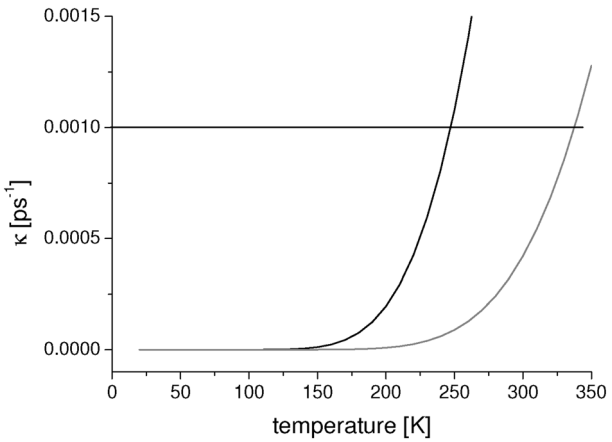

Fig. 3 Relaxation frequencies κ_{FWM} obtained by the fitting of the MDSs of Fig. 1 using eqn (5) and (6) (*h*AChE in black, *h*BChE in red). A horizontal straight line was added in the figure as guide to the eyes. It corresponds to the time resolution of IN16 of about 1 ns *i.e.* a frequency of 0.001 ps^{-1}.

close to those of $E_a^{\ddagger}$. Below the kinetic transition temperature, that approximately corresponds to about the end of the temperature range for the dynamics study, *h*AChE displays a larger negative entropy contribution to free energy of activation that is nearly 3 times that of *h*BChE (Table 2). This may suggest a very loose structure for *h*AChE and a high degree of ordering of the protein and the reactant water molecule in the transition state, in agreement with the high flexibility of *h*AChE and an important contribution of more faster local motion in the function of this protein.

It is certainly too early to conclude in a general manner for all enzymes, as only very little is known about the relation between flexibility and enzymatic activity at large and the present paper underlines some of the difficulties related to such studies. However, when taking carefully into account instrumental resolution effects into the fits, one is able to extract reliable values about thermodynamic parameters and to compare them with characteristics obtained from kinetic measurements as shown above. There exist some hints in recent publications (for instance in Kneller[42] or Henzler-Wildman and Kern[43]) that different time scales of dynamics are linked and our work is an indication for that, but it should be reinforced by further studies on other biological systems.

Acknowledgements

We gratefully acknowledge fruitful discussions with F. Natali, G. Kneller, G. Zaccai, D. Bicout, the ILL for allocation of beam time and the financing of the DGA under contract number REI no. 2009340023. This work is supported by an AINSE Research Fellowship (M. Tehei) and an AINSE PGRA (F. Hill). M. Trapp was supported by a PhD scholarship from the French Ministry for Research and Technology. F. Nachon acknowledges funding from the Agence Nationale de la Recherche (ANR; project number ANR-09-BLAN-0192-04). M. Tehei acknowledges the financial support from the Access to Major Research Facilities Program which is a component of the International Science Linkages Program established under the Australian Government's innovation statement, Backing Australia's Ability.

References

1 O. Kwasnieski, L. Verdier, M. Malacria and E. Derat, *J. Phys. Chem. B*, 2009, **113**, 10001–10007.
2 P. Masson and O. Lockridge, *Arch. Biochem. Biophys.*, 2010, **494**, 107–120.
3 F. Nachon, P. Masson, Y. Nicolet, O. Lockridge and J. Fontecilla Camps, *Comparison of the structures of butyrylcholinesterase and acetylcholinesterase*, in *Cholinesterases and Cholinesterase Inhibitors: Basic, Preclinical and Clinical Aspects*, Martin Bunitz, London, 2003, pp. 39–54.
4 J. Sussman, M. Harel, F. Frolow, C. Oefner, A. Goldman, L. Toker and I. Silman, *Science*, 1991, **253**, 872–879.
5 S. V. Lushchekina, A. V. Nemukhin, D. I. Morozov and S. D. Varfolomeev, *Chem.-Biol. Interact.*, 2010, **187**, 59–63.
6 L. Fang, Y. Pan, J. L. Muzyka and C.-G. Zhan, *J. Phys. Chem. B*, 2011, **115**, 8797–8805.
7 Y. Nicolet, O. Lockridge, P. Masson, J. Fontecilla-Camps and F. Nachon, *J. Biol. Chem.*, 2003, **278**, 41141–41147.
8 G. Kryger, M. Harel, K. Giles, L. Toker, B. Velan, A. Lazar, C. Kronman, D. Barak, N. Ariel, A. Shafferman, I. Silman and J. L. Sussman, *Acta Crystallogr., Sect. D: Biol. Crystallogr.*, 2000, **56**, 1385–1394.
9 E. Carletti, J.-P. Colletier, F. Dupeux, M. Trovaslet, P. Masson and F. Nachon, *J. Med. Chem.*, 2010, **53**, 4002–4008.
10 H. Dvir, I. Silman, M. Harel, T. L. Rosenberry and J. L. Sussman, *Chem.-Biol. Interact.*, 2010, **187**, 10–22.
11 F. Nachon, Y. Nicolet, N. Viguié, P. Masson, J. C. Fontecilla-Camps and O. Lockridge, *Eur. J. Biochem.*, 2002, **269**, 630–637.
12 R. Daniel, R. Dunn, J. Finney and J. Smith, *Annu. Rev. Biophys. Biomol. Struct.*, 2003, **32**, 69–92.
13 A. Shafferman, D. Barak, D. Stein, C. Kronman, B. Velan, N. H. Greig and A. Ordentlich, *Chem.-Biol. Interact.*, 2008, **175**, 166–172.
14 T. L. Rosenberry and D. M. Scoggin, *J. Biol. Chem.*, 1984, **259**, 5643–5652.
15 F. Gabel, M. Weik, P. Masson, F. Renault, D. Fournier, L. Brochier, B. P. Doctor, A. Saxena, I. Silman and G. Zaccai, *Biophys. J.*, 2005, **89**, 3303–3311.
16 G. L. Ellman, K. Courtney, V. Andres jr and R. M. Featherstone, *Biochem. Pharmacol.*, 1961, **7**, 88–90, IN1, 91–95.
17 V. F. Sears, *Neutron News*, 1992, **3**, 26–37.
18 A. Rahman, K. S. Singwi and A. Sjölander, *Phys. Rev.*, 1962, **126**, 986–996.
19 V. Réat, G. Zaccai, C. Ferrand and C. Pfister, Biological Macromolecular Dynamcis, Proceedings of a Workshop on Inelastic and Quasielastic Neutron Scattering in Biology, 1997, pp. 117–122.

Published on 17 February 2012 on http://pubs.rsc.org | doi:10.1039/C2CP23817A
Downloaded by University of Wollongong on 22 August 2012

View Online

20 M. Tehei and G. Zaccai, *Biochim. Biophys. Acta, Gen. Subj.*, 2005, **1724**, 404–410.
21 P.-H. Yang and J. A. Rupley, *Biochemistry*, 1979, **18**, 2654–2661.
22 J. Roh, J. Curtis, S. Azzam, V. Novikov, I. Peral, Z. Chowdhuri, R. Gregory and A. Sokolov, *Biophys. J.*, 2006, **91**, 2573–2588.
23 V. Kurkal, R. Daniel, J. L. Finney, M. Tehei, R. Dunn and J. C. Smith, *Biophys. J.*, 2005, **89**, 1282–1287.
24 W. Doster, S. Cusack and W. Petry, *Nature*, 1989, **337**, 754–756.
25 G. Zaccai, *Science*, 2000, **288**, 1604–1607.
26 T. Becker, J. A. Hayward, J. L. Finney, R. M. Daniel and J. C. Smith, *Biophys. J.*, 2004, **87**, 1436–1444.
27 D. J. Bicout and G. Zaccai, *Biophys. J.*, 2001, **80**, 1115–1123.
28 F. Gabel, P. Masson, M.-T. Froment, B. Doctor, A. Saxena, I. Silman, G. Zaccai and M. Weik, *Biophys. J.*, 2009, **96**, 1489–1494.
29 J. Pieper, T. Hauß, A. Buchsteiner, K. Baczynski, K. Adamiak, R. E. Lechner and G. Renger, *Biochemistry*, 2007, **46**, 11398–11409.
30 K. Wood, A. Frolich, A. Paciaroni, M. Moulin, M. Hartlein, G. Zaccai, D. Tobias and M. Weik, *J. Am. Chem. Soc.*, 2008, **130**, 4586–4587.
31 M. Bée, *Quasielastic Neutron Scattering: Principles and Applications in Solid State Chemistry, Biology and Materials Science*, Adam Hilger, Philadelphia, 1988.
32 G. Karp, *Cell and Molecular Biology*, John Wiley & Sons Ltd, 2007.
33 P. Masson and C. Balny, *Biochim. Biophys. Acta, Protein Struct. Mol. Enzymol.*, 1986, **874**, 90–98.
34 A. Ferro and P. Masson, *Biochim. Biophys. Acta, Protein Struct. Mol. Enzymol.*, 1987, **916**, 193–199.
35 K. R. Dave, A. R. Syal and S. S. Katyare, *Z. Naturforsch., C: Biosci.*, 2000, **55**, 100–108.
36 I. B. Wilson and E. Cabib, *J. Am. Chem. Soc.*, 1956, **78**, 202–207.
37 A. Stadler, I. Digel, J. Embs, T. Unruh, M. Tehei, G. Zaccai, G. Büldt and G. Artmann, *Biophys. J.*, 2009, **96**, 5073–5081.
38 M. Monkenbusch, D. Richter and R. Biehl, *ChemPhysChem*, 2010, **11**, 1188–1194.
39 F. Gabel and M.-C. Bellissent-Funel, *Biophys. J.*, 2007, **92**, 4054–4063.
40 C. Kronman, T. Chitlaru, E. Elhanany, B. Velan and A. Shafferman, *J. Biol. Chem.*, 2000, **275**, 29488–29502.
41 T. Chitlaru, C. Kronman, B. Velan and A. Shafferman, *Biochem. J.*, 2002, **363**, 619–631.
42 G. R. Kneller, *Phys. Chem. Chem. Phys.*, 2005, **7**, 2641–2655.
43 K. Henzler-Wildman and D. Kern, *Nature*, 2007, **450**, 964–972.

Published on 17 February 2012 on http://pubs.rsc.org | doi:10.1039/C2CP23817A
Downloaded by University of Wollongong on 22 August 2012

 This journal is © the Owner Societies 2012